ENERGY EXPLORATION & EXPLOITATION · Volume 29 · Number 6 · 2011 pp. 759–776

Influence and sensitivity study of matrix shrinkage and swelling on enhanced coalbed methane production and CO_2 sequestration with mixed gas injection

Fengde Zhou[1, 2], Guangqing Yao[1], Zhonghua Tang[3] and Oyinkepreye D. Orodu[4*]

[1]*Key Laboratory of Tectonics and Petroleum Resources (China University of Geosciences), Ministry of Education, Wuhan, Hubei 430074, China*

[2]*School of Petroleum Engineering, University of New South Wales, Sydney, NSW, 2052, Australia*

[3]*Faculty of Environment, China University of Geosciences, Wuhan, Hubei 430074, China*

[4]*Department of Petroleum Engineering, Covenant University, Ota PMB 1023, Ogun State, Nigeria*

(Received 19 July 2011; accepted 26 October 2011)

Abstract

Matrix compressibility, shrinkage and swelling can cause profound changes in porosity and permeability of coalbed during gas sorption and desorption. These factors affect the distribution of pressure, methane production and CO_2 sequestration.

This paper compares the effects of cleat compression and matrix shrinkage and swelling models with the injection of different compositional gas mixtures (CO_2 and N_2). It shows that well performance, pressure distribution and properties of the seam are strongly affected by matrix shrinkage and swelling. Matrix shrinkage and swelling also affects net present value of the enhanced coalbed methane recovery scheme. In order to select the best enhanced coalbed methane recovery schemes, economic evaluation and sensitivity studies are necessary.

Keywords: Shrinkage and swelling, Mixed gas injection, Economic evaluation, Sensitivity study

1. INTRODUCTION

Permeability is recognized as one of the most important parameters for coalbed methane (CBM) production. Both porosity and permeability of coalbed change during primary and enhanced methane recovery, due to changes in stresses of coalbed. Gayer

* Author for corresponding. Email: david.orodu@covenantuniversity.edu.ng

and Harris (1996) presented schematically the geomechanical parameters that are affected during CH_4 production and CO_2/N_2 injection. It shows that when pore pressure (P_f) decreases (a production process), the cleat-compression term (ε_p) is positive, while the matrix-shrinkage term (ε_s) is negative. Cleat-compression and matrix-shrinkage are two distinct phenomena, known to be associated with pressure depletion and gas desorption, with opposing effects on coal permeability. So, a suitable simulator which accounts for the changes of different stresses is vital for CBM production.

During primary recovery of methane, coal shrinks with gas desorption (Shi and Durucan, 2004; Shi and Durucan, 2005). The permeability may reduce during drainage with low shrinkage, but it may increases in case of a high shrinkage (Gray, 1987).

During enhanced methane recovery/CO_2 sequestration in coal, adsorption of CO_2, which has a greater sorption capacity than methane, would cause matrix swelling and thus, in contrast to gas desorption could have a detrimental impact on cleat permeability of coal. A large number of researchers have used different models to evaluate matrix shrinkage/swelling with CO_2 injection (Siriwardane *et al*., 2006; Gorucu *et al*., 2007; Mazumder and Wolf, 2008; Balan and Gunrah, 2009; Durucan and Shi, 2009; Pan and Connell, 2009; Siriwardane *et al*., 2009). For the injection of gas mixture, the production/injection performance, the pressure distribution, the porosity and permeability variation, are more complex than pure gas injection (Durucan and Shi, 2009).

Several permeability models have been studied (Durucan and Edwards, 1986; Gray, 1987; Mckee *et al*., 1987; Sawyer *et al*., 1990; Seidle *et al*., 1992; Palmer and Mansoori, 1998; Shi and Durucan, 2004; Shi and Durucan, 2005; Zeng *et al*., 2009; Shu *et al*., 2010). Among them, two models have widely been used, one is pressure based permeability model (Palmer and Mansoori, 1998; Balan and Gumrah, 2009) and the other is a gas concentration based model (Shi and Durucan, 2004; Shi and Durucan, 2005; Durucan and Shi, 2009).

This paper compares the production and injection performance, and changes in porosity and permeability simulated with matrix shrinkage/swelling model and non-matrix shrinkage/swelling model, with pure and mixed CO_2/N_2 as injectant. Furthermore, it studies the sensitivity of economic and mechanical parameters on the injection of different gas mixtures with shrinkage and swelling (SS) model.

2. DESCRIPTION OF THE STUDY AREA

Qinshui basin is one of the key CBM production districts in China. The area of Qinshui Basin is about 29,500 km^2, and estimated storage of CBM is $10.9\times10^{12}m^3$ for depth less than 1,500 m and 36.8×10^{12} m^3 for depth less than 2,000 m. The main coal seams are Seam No. 5 and Seam No. 8. Seam No. 8 is the focus of this study. The seam is deposited at a subsurface depth of 505 m (Fig. 1). The CBM reservoir is unsaturated with an initial and desorption pressure of 4,850 kPa and 2,400 kPa, respectively. The thickness is 3.5–4.0 m. The core porosity and permeability are 1.8% and 12 md, respectively. Table 1 shows the fluid and rock characteristics and Table 2 shows the Langmuir isotherm parameters and Table 3 shows the relative permeability used in the

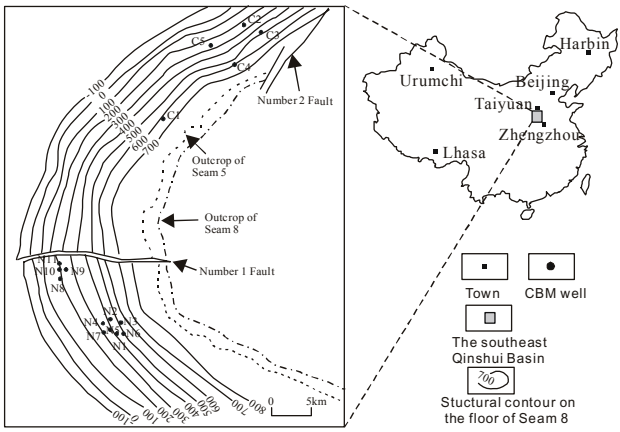

Figure 1. Location of Hedong area and structure contours on the floor of Seam No. 8 (After Wang, 2007).

Table 1. Fluid and rock properties.

Parameter	Value	Unit
Water saturation, *Sw*	100	%
Temperature, *T*	50	Celsius
Water density, ρ_w	998	kg/m^3
Water formation factor, Bw	1.01	Dimensionless
Water viscosity, μ	0.447	cp
Water compressibility, C_w	4.1	10^{-8} kPa^{-1}
Porosity compressibility, c_p	1.9	10^{-6} kPa^{-1}
Matrix shrinkage coefficient, c_m	6	10^{-6} kPa^{-1}
Bulk density, ρ_R	1,356	kg/m^3

Table 2. Isotherm Langmuir parameters.

Parameter	CH_4	CO_2	N_2*	Unit
Langmuir pressure, P_L	1,350	600	1,500	kPa
Langmuir adsorbed gas content, V_L	25	35	10	m^3/t
Desorption pressure, P_{des}	2,400			kPa
Initial gas content, C_0	16	0	0	m^3/t
Desorption time, τ	3	2.3	5	days

*The parameters of N_2 were assumed

simulation model. The strain constants for maximum stress (ε_{max}), Poisson's ratio (v), Young's modulus (E) and cleat compressibility are 0.02, 0.35, 2.8 GPa and 9×10^{-5} kPa^{-1}, respectively. The SIMEDWin simulator is used in this study and the numerical model is described in the appendix.

Table 3. Relative permeability of water and gas used in simulation.

Water saturation, S_w	Gas phase relative permeability, K_{rg}	Water phase relative permeability, K_{rw}
0.00	0.000	1.000
0.20	0.001	0.896
0.35	0.007	0.835
0.45	0.021	0.771
0.61	0.067	0.451
0.74	0.210	0.119
0.82	0.365	0.029
0.91	0.602	0.009
0.96	0.789	0.001
1.00	1.000	0.000

3. COAL COMPRESSIBILITY, SHRINKAGE AND SWELLING MODEL

3.1 Porosity compression model (PCM)

The porosity-compression model (PCM) is the model that illustrates the effect of compression on porosity, neglecting matrix shrinkage. The relationship between porosity, compressibility and pressure is

$$\phi = \phi_0 \cdot (1 + c_p(p - p_0)) \tag{1}$$

where c_p is matrix compressibility in kPa^{-1}, P_0 is initial pressure in kPa; $\varnothing_o$ is the porosity at initial pressure in fraction, p is reservoir pressure in kPa, $\varnothing$ is the porosity at pressure p in fraction.

The relationship between permeability and porosity is described by

$$k = k_0 \cdot \left(\frac{\phi}{\phi_0} \right)^3 \tag{2}$$

where k is permeability at pressure p in md, k_0 is the permeability at pressure p_0 in md.

3.2. Shi-Durucan model (SDM)

This model (Shi and Durucan, 2004; Shi and Durucan, 2005) is similar to Gray's model (Gray *et al*., 1987) in that, change in the cleat permeability during pressure drawdown is controlled by the prevailing effective horizontal stresses. However, there is an important difference between these two models. The volumetric matrix shrinkage in the present model is considered proportional to the volume of desorbed gas rather than to reduction in the equivalent sorption pressure. The equation is

$$\sigma - \sigma_0 = -\frac{\nu}{1-\nu}(p - p_0) + \frac{E\alpha_s V_L}{3(1-\nu)}\left(\frac{bp}{bp+1} - \frac{bp_0}{bp_0+1} \right) \tag{3}$$

where ν is Poisson's ratio in fraction, p is reservoir pressure in kPa, p_0 is the initial reservoir pressure in kPa, α_s is the volumetric-shrinkage coefficient in t/m^3, E is

Young's modulus in GPa, b is Langmuir constant in kPa^{-1}, V_L is Langmuir volume in m^3/t, σ is effective horizontal stress in kPa and σ_o is initial effective horizontal stress in kPa.

In SIMEDWin (CBM numerical simulator), change in horizontal effective stress is given by the following equations

$$\sigma - \sigma_0 = -\frac{\nu}{1-\nu}(P - P_0) + \frac{E}{3(1-\nu)}(\varepsilon(C_{tot}) - \varepsilon(C_{tot0})) \tag{4}$$

$$\varepsilon = \varepsilon_{\max} C_{tot} / VL_{\max} \tag{5}$$

$$C_{tot} = \sum_{j=1}^{n} C_j = \sum_{j=1}^{n} \frac{V_{Lj} p_j b_j}{1 + \sum_{j=1}^{n} p_j b_j} \tag{6}$$

where C_{tot} is total gas content in m^3/t, C_{tot0} is original total gas content at initial reservoir pressure in m^3/t, $\varepsilon_{\max}$ is maximum strain at $VL_{\max}$ in dimensionless, $VL_{\max}$ is the maximum Langmuir volume of the gas in mixture in m^3/t, j is gas component, p_j is the partial free gas pressure in kPa, b_j is Langmuir constant for gas component j in kPa^{-1}.

Permeability is modeled after Seidle model (Seidle *et al*., 1992). The cleat permeability varies exponentially with change in the effective horizontal stress as

$$k = k_0 \cdot e^{-3c_f(\sigma - \sigma_0)} \tag{7}$$

where c_f is cleat-volume compressibility with respect to changes in the effective horizontal stress normal to cleats in kPa^{-1}, and k_0 is initial coalbed permeability in md.

4. SIMULATION RESULTS WITH POROSITY COMPRESSION MODEL (PCM)

4.1. Comparison of production

For PCM, porosity and permeability have no apparent change for matrix shrinkage and swelling, and the effect of compressibility on porosity is quite low. The different components of mixed gas have no obvious effect on cumulative CH_4 production. Results show that cumulative CH_4 production is highest with pure N_2 injection followed by the decreasing trend of mixed and single gas injection of 25% CO_2/75% N_2, pure CO_2, 50% CO_2/50% N_2 and 75% CO_2/25% N_2. However, the cumulative CH_4 production of enhanced coalbed methane (ECBM) is about 2.8 times that of primary cumulative CH_4 production (Fig. 2A).

The peak CH_4 production rate decreases with decrease in N_2 gas content, but there is a longer period of peak CH_4 production rate with pure CO_2 injection (Fig. 2B). The highest peak CH_4 production rate for ECBM is 8 times that of primary CH_4 production rate. The produced CH_4 mole fraction in the production well is inversely proportional to the CH_4 production rate (Fig. 2C).

Geological storage of anthropogenic CO_2 is also an important part of coalbed exploitation. Figure 2D shows that cumulative storage of CO_2 increases with increase in CO_2 component of the mixed gas during ECMB. The cumulative storage of CO_2 with pure CO_2 injection is about 3 times that of 25% CO_2/75% N_2 gas injection.

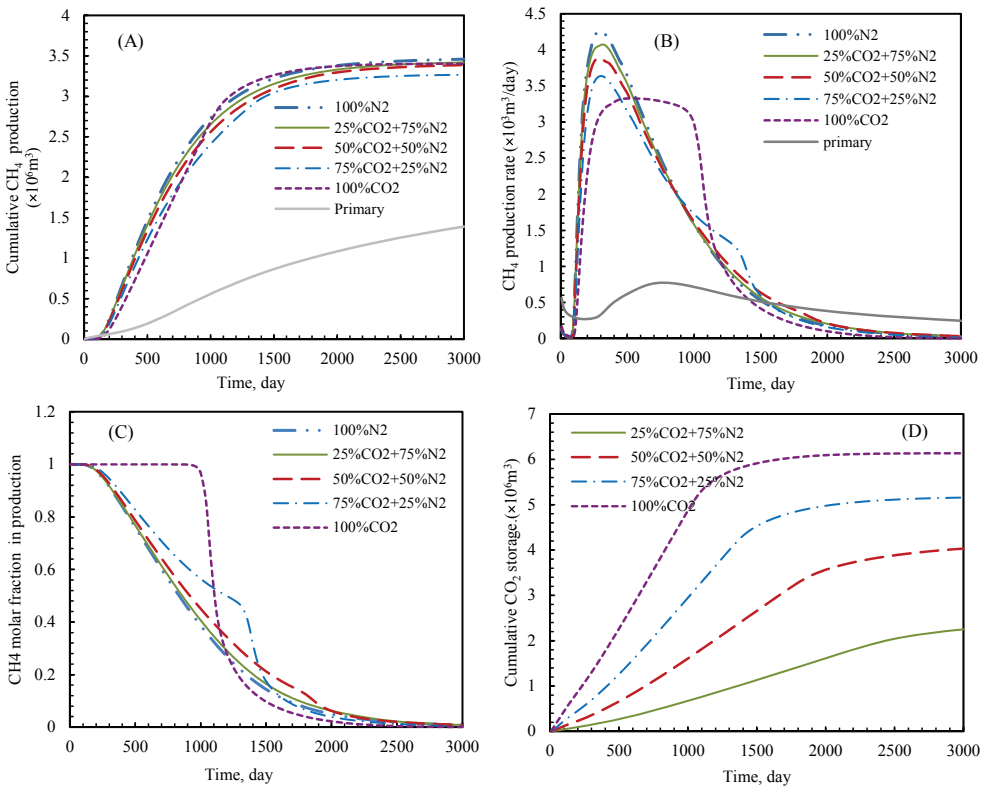

Figure 2. (A) Comparison of CH_4 cumulative production with different mixed-gas injection; (B) Comparison of CH_4 production rate with different mixed-gas injection; (C) Comparison of CH_4 molar fraction in production with different injectant; (D) Comparison of accumulative CO_2 storage with different mixed-gas injection.

4.2. Comparison of pressure distribution

The simulated pressure distribution from injection well to production well on 1,440th day is shown in Figure 3A. The results demonstrate negligible difference in pressure distributions with injection of different gas mixtures. However, the pressure distribution for the injection of 50% CO_2/25% N_2 gas was the lowest.

4.3. Comparison of gas concentration distribution

Figure 3B presents the distribution of adsorbed CH_4 diagonally from injection well to production well at 1,440 days. The adsorbed CH_4 content is negligible in pure or mixed gas flood zone, which illustrates the gas flow speed. The size of the area having residual CH_4 at 1,440 days at the vicinity of the production well decreases in the order of 25% CO_2/75% N_2, pure N_2, 50% CO_2/50% N_2, 75% CO_2/25% N_2, and pure CO_2. But the scheme with 50% CO_2/50% N_2 gas injection has the highest residual CH_4.

Figure 3C presents the distribution of adsorbed CO_2 diagonally from injection well to production well on 1,440th day. It shows that the adsorbed CO_2 content is

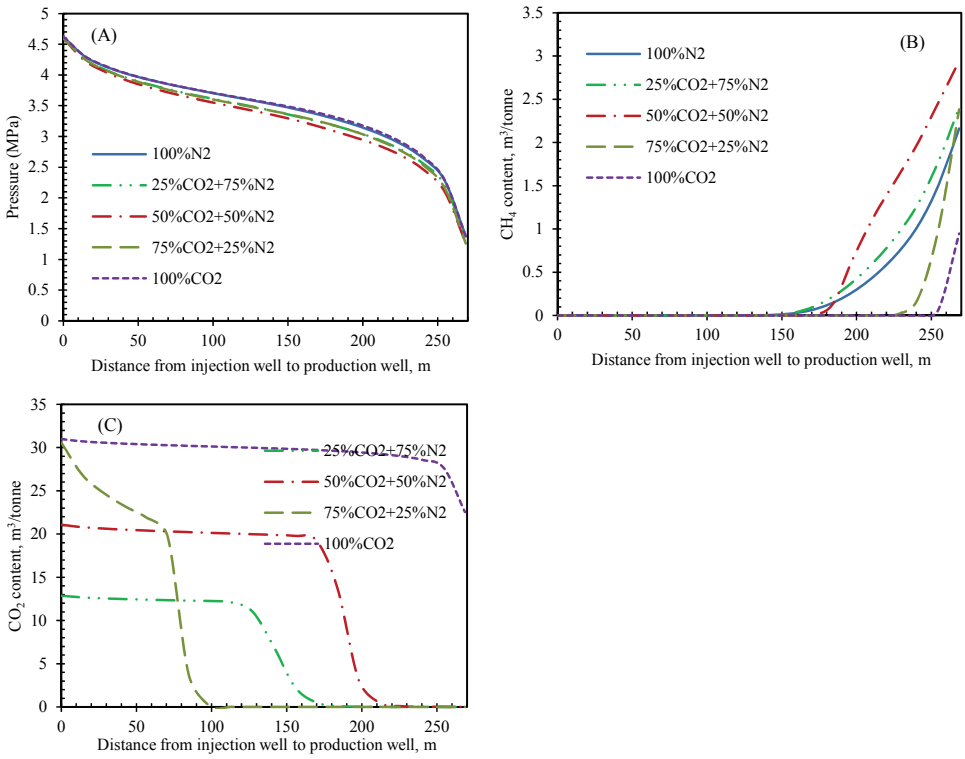

Figure 3. (A) Comparison of reservoir pressure from injection well (0 m) to production well (270 m) with different mixed-gas injection; (B) Grid block adsorbed CH_4 concentration from injection well (0 m) to production well (270 m) on 1,440th day with different mixed-gas injection; (C) Grid block adsorbed CO_2 concentration from injection well (0 m) to production well (270 m) on 1,440th day, with different mixed-gas injection.

almost the same, 30 m^3/ton, from injection well to production well, except at 20 m from the production well on 1,440th day, with pure CO_2 injection. The CO_2 distribution area is within 100 m, 170 m and 220 m of the injection well vicinity for mixed gas injection of 75% CO_2/25% N_2, 25% CO_2/75% N_2, and 25% CO_2/75% N_2, respectively.

5. SIMULATION RESULTS WITH MATRIX SHRINKAGE/SWELLING MODEL

5.1. Comparison of production

Injection of N_2 or CO_2 can reduce the partial pressure of methane in seam, which promotes methane desorption from coal matrix (Puri and Yee, 1990; Durucan and Shi, 2009). At same time, the different sorption capacity (described by Langmuir volume, V_L) may cause different matrix shrinkage and swelling. Since CO_2 has a greater swelling coefficient than CH_4, and CH_4 greater than that of N_2, the well performance, pressure

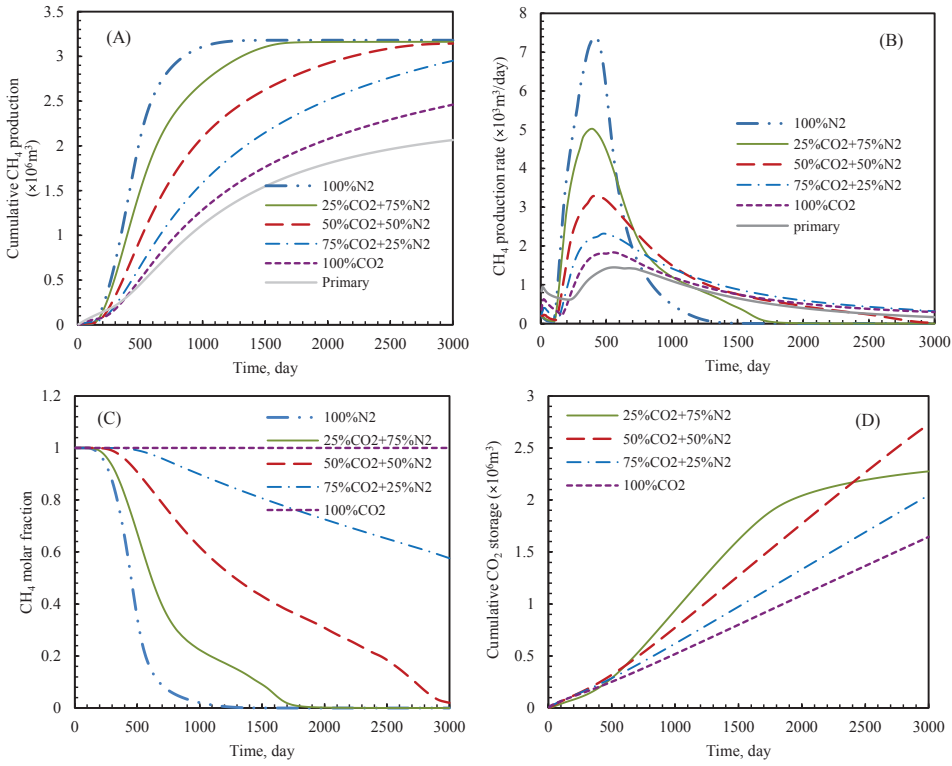

Figure 4. (A) Comparison of CH_4 cumulative production with different mixed-gas injection; (B) Comparison of CH_4 production rate with different mixed-gas injection; (C) Comparison of CH_4 molar fraction in production with different injectant; (D) Comparison of cumulative CO_2 storage with different mixed-gas injection.

distribution, and changes of porosity and permeability will depend on gas components. These occur, especially for strong swelling and shrinkage coal seam.

It is observed that cumulative CH_4 production decreases with decrease of N_2 content in the injected gas mixture within 3 years. As the injected mixture is enriched in N_2, an increasingly larger portion of the methane in place can be recovered (Fig. 4A). Peak CH_4 production rate also decreases with decrease of N_2 content in the injected gas mixture. But the time of peak CH_4 production rate is similar for all gas injection schemes (Fig. 4B). The produced CH_4 mole percent is almost 100% within 3,000 days with pure CO_2 injection, and decreases with decrease of CO_2 content in the mixed gas. It is because the increasing component of N_2 in mixed gas will increase the reservoir permeability which caused earlier injectant breakthrough (Fig. 4C).

Prior to the 2,300th day, cumulative CO_2 storage decreased with increasing CO_2 content in the injected gas stream. This trend changed after the 2,300th day for 25% CO_2/75% N_2 gas injection as produced CO_2 exceeded injected CO_2. At the end of

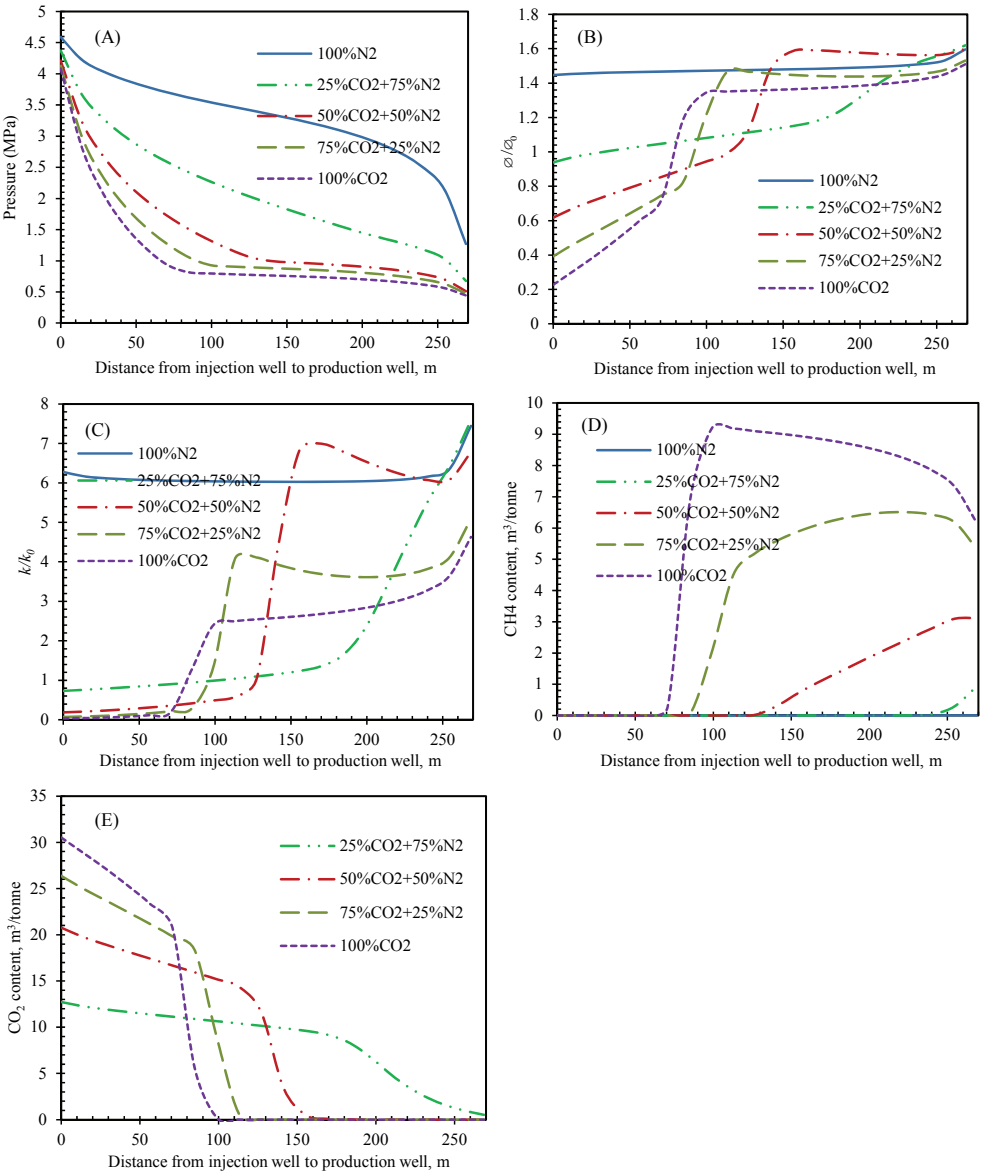

Figure 5. (A) Variation of reservoir pressure from injection well (0 m) to production well (270 m) with different mixed-gas injection; (B) Variation of porosity ratio from injection well to production well on 1,440th day with different mixed-gas injection; (C) Variation of permeability distribution from injection well (0 m) to production well (270 m) on 1,440th day with different mixed-gas injection; (D) Variation of CH_4 content with different mixed-gas injection diagonally from injection well to production well; (E) Variation of CO_2 content with different mixed-gas injection diagonally from injection well to production well.

simulation (3000th day), cumulative CO_2 storage was highest for 50% CO_2/50% N_2 followed by 25% CO_2/75% N_2, and 75% CO_2/25% N_2, and lowest for pure CO_2 (Fig. 4D).

5.2. Comparison of pressure distribution

Figure 5A shows the simulated pressure distribution diagonally from the injection well (Left in X-axis) to the production well (Right in X-axis). Results show that pressure decreases with increase in N_2 content in the injectant. It is because N_2 injection leads to coal shrinkage since it has less adsorption capacity than CH_4. Then the shrinkage leads to increasing coal permeability. The incremental permeability is higher with higher N_2 component in injectant.

5.3. Comparison of variation of porosity and permeability

For mixed gas (CO_2/N_2) injection, there are three zones between the injection well and the production well, 2-mixed gas injection zone, 3-mixed gas flow zone (transition zone), and CH_4 flow zone. Due to the different shrinkage and swelling characteristics of the different gases in the injection mixture, porosity and permeability are profoundly different with SDM (Fig. 6).

Figure 5B shows the comparison of porosity distribution from the injection well to the production well at 1,440 days with injection of different gas mixtures. For pure N_2 injection, the porosity ratio ($\varnothing/\varnothing_o$) is almost the same from the injection well to the production well, 1.44, except the CH_4 flow zone is 1.6. With the decrease of N_2 content in the gas mixture, the three-mixed-gas zone moves from the vicinity of production well to the injection well. In the mixed gas injection zone, the porosity ratio decreases with decrease of N_2 content in the injected gas mixture. The peak porosity ratio of pure N_2 injection is almost the same with 25% CO_2/75% N_2, and 50% CO_2/50% N_2 injection, and higher than that of 75% CO_2/25% N_2 and pure CO_2 injection. The pattern of variation of permeability ratio (k/k_o) is similar to the porosity pattern (Fig. 5C).

5.4. Comparison of gas concentration distribution

The gas content is also different in the above mentioned three zones. For pure N_2 injection, there is no CH_4 residual, and for 25% CO_2/75% N_2 injection, there is minute

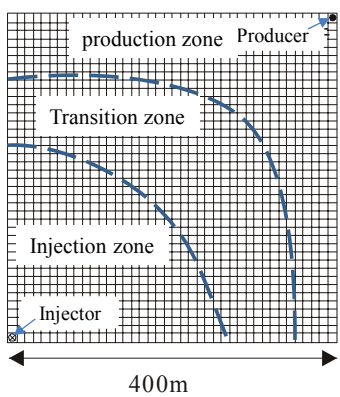

Figure 6. Scheme diagram shows the distribution of three zones for gas flow.

CH_4 residual in the vicinity of the production well. Simulation results of 50% CO_2/50% N_2, 75% CO_2/25% N_2 and pure CO_2 gas injection show that CH_4 content increases with increase in CO_2 content of the injected mixed gas stream at the same block in mixed gas flow zone and CH_4 flow zone (Fig. 5D).

Figure 5E shows the CO_2 content from the injection well to the production well on 1,440th day. It shows an inverse trend with permeability ratio in Figure 5C.

6. ECONOMIC EVALUATION AND SENSITIVITY STUDY

6.1. Equations and parameters

Net present value (NPV) is often used as an economic evaluation parameter (Gorucu *et al*., 2007) that reflects the feasibility of a production scheme and its profitability. In this study, the NPV equation is

$$NPV = \sum_{n=0}^{N} \frac{CF_t}{(1+i)^n} \tag{8}$$

$$CF_t = C_s + C_y + C_w + C_g + I_{CH_4} + I_{cCO2} \tag{9}$$

where CF_t is the total cashflow in n^{th} year in 10^3USD, C_s is the startup cost in 10^3USD, C_y is annual operating and capital cost in 10^3USD, C_w is water disposal cost in 10^3USD, C_g is the cost of gas injection in 10^3USD, I_{CH4} is CH_4 income in 10^3USD, I_{cCO_2} is CO_2 storage income in 10^3USD, N is the planned years of the project in year and, i is the discount rate in fraction.

Table 4 shows the startup cost (this includes drilling, surface equipments, downhole equipment, pipeline cost, etc.) and operating cost. The cost of gas injection well is a quarter of a single well because the simulation study area is a quarter of a five-spot pattern.

6.2. Sensitivity on gas price

In order to study the sensitivity of parameters, the duration of simulation was prolonged from 3,000 days to 7,300 days.

Table 4. Economic parameters that were used in the analysis (After Gorucu *et al*., 2007).

	Cost type	Cost per vertical wells ($\times 10^3$ USD)	Total cost ($\times 10^3$ USD)
Startup costs	Drilling	94	94
	Surface Equipment	19	19
	Downhole Equipment	8	8
	Pipeline costs	2	2
	MMV (at 10%)	12	12
		Total startup	**135**
Yearly costs	Operations and Maintenance*	10	12.5
	MMV (at 10%)		1.25
		Total startup	**13.75**

* Reasonable changed after Gorucu *et al*. (2007)

Table 5. Comparison of NPV with different gas injection and price ratio of N_2 over CO_2.

Gas injection	Ratio of N_2 cost price over CO_2 cost price			
	1 time	2 times	3 times	4 times
Pure N2	409/7 *	189/6	11.4/6	−127/5
25% CO_2/75% N2	360/11	202/9	67.5/8	−50.6/7
50% CO_2/50% N2	269/>20	194/17	124/15	58.5/13
75% CO_2/25% N2	169/>20	148/>20	127/>20	107/>20
Pure CO_2	114/>20	114>20	114/>20	114/>20

* 409/7 is NPV(10^3USD) / Life of project (years)

The sensitivity of gas prices, in this study, includes CH_4 price, CO_2 cost and N_2 cost, and CO_2 storage credit. The CO_2 storage credit can be treated to decrease the CO_2 cost. Water-disposal cost and discount rate are 2.5USD/m^3 and 0.12 respectively. The N_2 cost varies from 0.01USD/m^3 to 1USD/m^3.

Based on a constant CH_4 price of 0.14USD/m^3 and CO_2 cost of 0.04 USD/m^3, results show that the best injection schemes are pure N_2, 25% CO_2/75% N_2, 75% CO_2/25% N_2, and pure CO_2 (Table 5) when the cost of N_2 is 1, 2, 3 and 4 times that of the CO_2 cost, respectively. Pure CO_2 injection scheme will be the best when the N_2 cost is over 4 times that of the CO_2 cost.

Figure 7 shows the results for N_2 cost of 0.08USD/m^3, varied CH_4 price of 0.11USD/m^3, 0.14 USD/m^3, and 0.18 USD/m^3, and varied CO_2 cost of 0.02 USD/m^3, 0.04 USD/m^3, and 0.06 USD/m^3, respectively. When the price of CH_4 is 0.11USD/m^3, the best schemes are 50% CO_2/50% N_2, 50% CO_2/50% N_2, and pure N_2 injection respectively, and the corresponding NPVs are 43×10^3USD, 9.3×10^3USD and

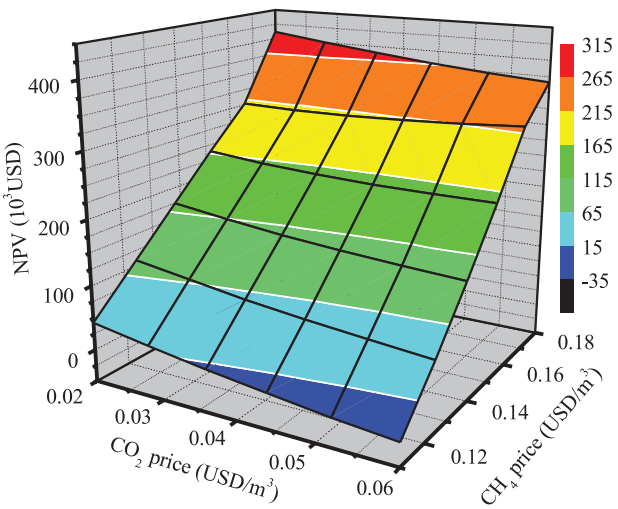

Figure 7. Influence of CH_4 and CO_2 price on NPV of the best scheme.

Table 6. Comparison of NPV with different mechanical parameters.

Scenario	Poisson's ratio, v	Young's modulus, E (GPa)	Economical life of project (years)	NPV (10^3USD)
1	0.17	1.4GPa	10	154.8
2	0.17	2.8GPa	8	196.5
3	0.17	4.2GPa	7	276.4
4	0.35	1.4GPa	11	101.0
5	0.35	2.8GPa	9	160.0
6	0.35	4.2GPa	7	323.1
7	0.53	1.4GPa	13	10.2
8	0.53	2.8GPa	10	112.0
9	0.53	4.2GPa	7	415.6

-14.9×10^3USD, and the best periods are 16, 14 and 6 years respectively. When the price of CH_4 is 0.14USD/m^3, the best schemes are 25% CO_2/75% N_2, 25% CO_2/75% N_2, and pure N_2 injection respectively, and the corresponding NPVs are 184×10^3USD, 160×10^3USD and 148×10^3USD, and the best periods are 9, 9 and 6 years respectively. When the price of CH_4 is 0.18USD/m^3, the best schemes are 25% CO_2/75% N_2, 25% CO_2/75% N_2, and pure N_2 injection respectively, and the corresponding NPVs are 366×10^3USD, 385×10^3USD and 412×10^3USD, and the best periods are 6, 10 and 10 years respectively.

6.3. Sensitivity on mechanical properties

To simplify the study, the CH_4 price, CO_2 cost and N_2 cost is 0.14USD/m^3, 0.04 USD/m^3 and 0.08 USD/m^3, respectively. We select the scheme with 25%CO_2/75% N_2 injection for sensitivity study. Based on this scheme, the sensitivity of Poisson's Ratio and Young's Modulus on NPV is studied. The Poisson's Ratio and Young's Modulus were both varied ±50% from the base value of 0.35 and 2.8GPa, respectively.

Table 6 shows the relationship between NPV of cumulative CH_4 production and Poisson's Ratio and Young's Modulus. Equation (4) shows that effective stress has a positive relationship with Young's Modulus.

7. DISCUSSION

The impact of models used to predict performance of enhanced coalbed methane production, the geomechanical and reservoir properties of the seam and gas composition of injectant was investigated with the aim of economically optimizing methane gas recovery.

Reduced permeability based on matrix shrinkage and swelling will affect CH_4 production and CO_2 storage in coalbed seams. It should be evaluated for different schemes before it is used for ECBM, so as to evaluate the influence of seam geomechanical parameters (Gorucu *et al.*, 2007), injection of gas mixture (Durucan and Shi, 2009), seam properties, and adsorption models (Pan and Connell, 2009).

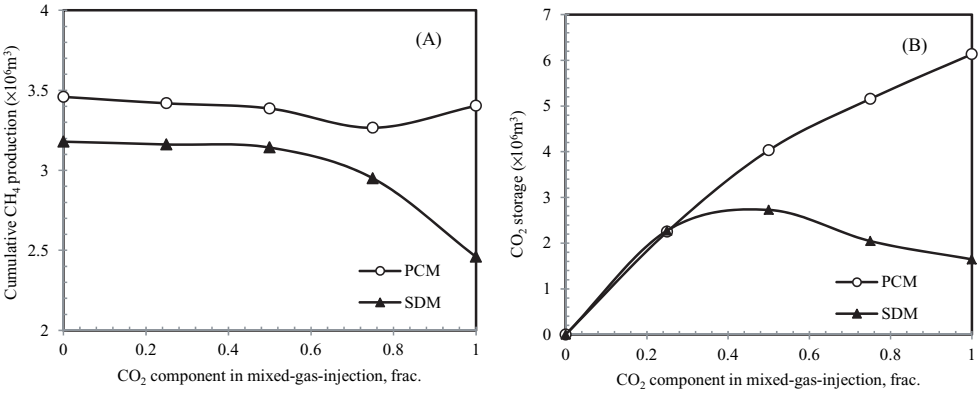

Figure 8. (A) Comparison of cumulative CH_4 production versus CO_2 content in gas mixture injection with PCM and SDM; (B) Comparison of cumulative CO_2 storage versus CO_2 content in gas mixture injection with PCM and SDM within period 3,000 days.

It is confirmed that N_2 flooding can reverse permeability reduction due to matrix swelling (Shi *et al*., 2008). But pure N_2 and N_2 rich ECBM may affect CO_2 storage. Figure 8A and Figure 8B show that for negligible matrix shrinkage and swelling seam, pure CO_2 injection would not only result to similar CH_4 recovery but also the highest CO_2 sequestration. For strong matrix shrinkage and swelling coal, the injection of 50% CO_2/50% N_2 gas has the highest CO_2 storage capacity. The cumulative CH_4 production of PCM is higher than that of SDM. The scheme with pure N_2 injection has the highest cumulative CH_4 production for both non shrinkage/swelling and shrinkage/swelling model.

Figure 9 shows that CO_2 breakthrough distance from the injection well has a power law relationship with the CO_2 content in the injected gas mixture with SDM. But this equation will vary, depending on the properties of coalbed.

Moreover, coalbed methane production is a complex process, which is affected by not only the deformation of pore pressure, but also the shrinkage and swelling of adsorption and desorption. The effect of shrinkage and swelling on CH_4 production and CO_2 storage is also different for the injection of different gas mixtures. The NPV analysis can help to select the best scheme. But the results will be different when simulated with different Shrinkage/Swelling models.

8. CONCLUSIONS

This paper has studied the influence of matrix shrinkage and swelling on well performance and seam properties with the injection of gas mixture and different models. The major conclusions are given below:

There is a strong shrinkage and swelling effect on well performance and seam properties of the coal seam in Hedong Area, Qinshui Basin. For negligible matrix shrinkage and swelling coal seam, the best ECBM scheme is pure CO_2 injection, or the 50%CO_2/50%N_2 gas.

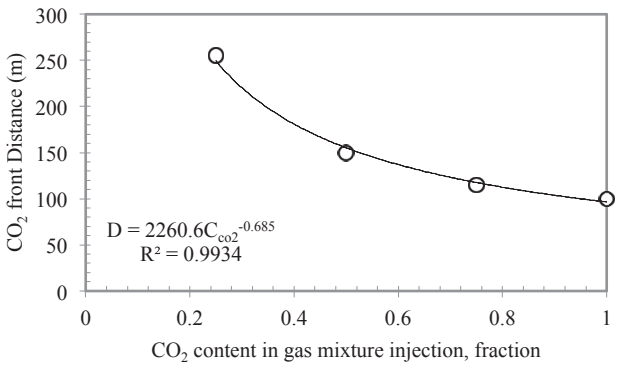

Figure 9. The relationship between CO_2 front distance and CO_2 content in injectant on 1,440th day.

In order to select an optimal ECBM scheme, economic and sensitivity study was based on Shi-Durucan model (SDM) thereby considering matrix shrinkage and swelling of coal seam. By using the SDM, decreasing N_2 content in injected mixed gas decreases cumulative CH_4 production. Based on sensitivity analysis, increasing the cost of N_2 from 1 to 4 times the cost of CO_2, the optimal scheme is in the decreasing order of pure N_2 injection, 25% CO_2/75% N_2, 50% CO_2/50% N_2, 75% CO_2/25% N_2 and pure CO_2 injection, respectively. Simulated cumulative CH_4 production and NPV have positive relationship with Young's modulus, and have specific relationship with Poison's ratio. The maximum NPV is proportional to Poison's ratio when Young's modulus equals to 1.4GPa and 2.8GPa, and inversely proportional to Poison's ratio when Young's modulus is 4.2GPa.

However, the economic evaluation of ECBM by gas injection is a complex process. More parameters should be considered if possible, such as the cost of produced gas separation, and the income from gas recycling.

ACKNOWLEDGEMENTS

The Project was supported by the Fundamental Research Funds for the Central Universities, China University of Geosciences (Wuhan) (CUGL100249) and TPR-2010-15. The authors would like to thank Prof. Val Pinczewski for the support of using the CBM simulator, SIMEDWin.

APPENDIX: DESCRIPTION OF RESERVOIR PROPERTIES USED IN SIMULATION STUDIES

Grid system (SECTION 4 and 5):

Cartesian (x-y-z) =20×20×1

Grid spacing for *x*,*y* and *z* direction (m): 10, 10 and 3.5

Grid system (SECTION 6 and 7):
Cartesian (x-y-z) =40×40×1
Grid spacing for *x*,*y* and *z* direction (m): 10, 10 and 4
Reference porosity: 1.8%
Reference permeability: 12md
Well locations:
Injection well: Grid (1, 1)
Production well (SECTION 4 and 5): Grid (20, 20)
Production well (SECTION 6 and 7): Grid (40, 40)
Well radius: =0.07 m
Well skin factor=0
Production well controlled by BHP=350 kPa
CO_2 injection under controlled by BHP=4,850 kPa

REFERENCES

Balan H.O. and Gumrah F., 2009. Assessment of shrinkage-swelling influences in coal seams using rank-dependent physical coal properties. *International Journal of Coal Geology* **77**, 203–213.

Durucan S. and Shi J.Q., 2009. A Improving the CO_2 well injectivity and enhance coalbed methane production performance in coal seams. *International Journal of Coal Geology* **77**, 214–221.

Durucan S. and Edwards J.S., 1986. The effects of stress and fracturing on permeability of coal. *Mining Sciences and Technology* **3**, 205.

Gayer R. and Harris I., 1996. Coalbed Methane and Coal Geology. London, Geological Society, pp. 204–212.

Gorucu F.B., Jikich S.A., Bromhal G.S., Sams W.N., Ertekin T. and Smith D.H., 2007. Effects of matrix shrinkage and swelling on the economics of enhanced-coalbed-methane production and CO_2 sequestration in coal. *SPE Reservoir Evaluation & Engineering* **10**(**4**), 382–392.

Gray I., 1987. Reservoir engineering in coal seams: Part 1- the physical process of gas storage and movement in coal seams. *SPE Reservoir Engineering* **2**(**1**), 28–34.

Mazumder S. and Wolf K.H., 2008. Differential swelling and permeability change of coal in response to CO_2 injection for ECBM. *International Journal of Coal Geology* **74**, 123–138.

McKee C.R., Bumb A.C. and Koenig R.A., 1987. Stress-dependent permeability and porosity of coal. In: Proceeding of coalbed methane symposium, Tuscaloosa, Alabama, November 16–19.

Palmer I. and Mansoori J., 1998. How permeability depends on stress and pore pressure in coalbeds: A new model. *SPE Reservoir Evaluation & Engineering* **1**(**6**), 539–544.

Pan Z.J. and Connell L.D., 2009. Comparison of adsorption models in reservoir simulation of enhanced coalbed methane recovery and CO_2 sequestration in coal. *International Journal of Greenhouse Gas Control* **3**, 77–89.

Puri R. and Yee D., 1990. Enhanced coalbed methane recovery. Paper 20732 presented at the SPE 65th Annual Technical Conference and Exhibition, New Orleans, LA, September 23–26.

Sawyer W.K., Paul G.W. and Schraufnagel R.A., 1990. Development and application of a 3D coalbed simulator. Paper CIM/SPE 90–119 presented at the SPE International Technical Meeting. Calgary, June 10–13.

Seidle J.P., Jeansonne M.W. and Erickson D.J., 1992. Application of matchstick geometry to stress dependent permeability in coals. Paper 24361 presented at the SPE Rocky Mountain Regional Meeting, Casper, Wyoming, May 18–21.

Shi J.Q. and Durucan S., 2004. Drawdown induced changes in permeability of coalbeds: A new interpretation of the reservoir response to primary recovery. *Transport in Porous Media* **56**, 1–16.

Shi J.Q. and Durucan S., 2005. A model for changes in coalbed permeability during primary and enhanced methane recovery. *SPE Reservoir Evaluation & Engineering* **8**(**4**), 291–299.

Shi J.Q., Durucan S. and Fujioka M., 2008. A reservoir simulation study of CO_2 injection and N_2 flooding at the Ishikari coalfield CO_2 storage pilot project, Japan. *Int. J. Greenhouse Gas Control* **2**, 47–57.

Shu J., Wang H., Cai D.S., Guo H., Zhu G.H., Zhu X.M. and Hu X.L., 2010. The secondary porosity and permeability characteristics of Tertiary strata and their origins, Liaodong Bay Basin, China. *Energy Exploration & Exploitation* **28(4)**, 207–222.

Siriwardane H.J., Gondle R.K. and Smith D.H., 2009. Shrinkage and swelling of coal induced by desorption and sorption of fluids: Theoretical model and interpretation of a field project. *International Journal of Coal Geology* **77**, 188–202.

Siriwardane H.J., Smith D.H., Gorucu F. and Erterkin T., 2006. Influence of shrinkage and swelling of coal on production of coalbed methane and sequestration of carbon dioxide. Paper 102767 presented at the SPE Annual Technical Conference and Exhibition, San Antonio, U.S.A., September 24–27.

Snow D.T., 1968. Rock fracture spacings, openings and porosities. *J. of Soil Mech. and Foundations Div*., 73–91.

Wang X.J., 2007. Influence of coal quality factors on seam permeability associated with coalbed methane production. Doctoral Thesis, University of New South Wales, Sydney, Australia, PP. 167.

Zeng L.B. and Liu H.T., 2009. The key geological factors influencing on development of low-permeability sandstone reservoirs: A case study of the Taizhao area in the Songliao Basin, China. *Energy Exploration & Exploitation* **27(6)**, 425–438.